SMAR 2017 – Fourth Conference on Smart Monitoring,
Assessment and Rehabilitation of Civil Structures

SMAR 2017

Ductility improvement of existing RC columns strengthened with CFRP

M. Del Zoppo[1], M. Di Ludovico[2], A. Balsamo[2] and A. Prota[2]

[1] University of Naples Parthenope, Naples, Italy
[2] University of Naples Federico II, Naples, Italy

ABSTRACT: Existing reinforced concrete (RC) columns, designed according to obsolete standards, often show premature failures due to shear-flexure interaction, longitudinal bars buckling or loss of bond when subjected to horizontal cyclic loads. This kind of failure modes significantly reduces the deformation capacity and the relevant ductility of existing RC columns and leads to poor performances during seismic events. In order to improve the seismic performance of existing RC columns, the use of fiber reinforcement polymers (FRP) is recognised as a reliable technique. However, the analytical prediction of the capacity of strengthened members is still a challenging task. In this work, four square RC columns with deformed bars, designed according to obsolete standards, were strengthened in the plastic hinge region with one and two plies of uniaxial CFRP sheets. The columns were tested under horizontal cyclic load combined with a constant compressive axial load. The performance of strengthened columns has been compared with an unstrengthened control column. The test results have been analysed and compared in terms of failure modes and ductility improvement. Particular attention has been focused on the strain distribution recorded on the CFRP strips; the strain profiles along the cross-section perimeter in case of axial load and bending moment interaction are presented and discussed in comparison with codes provisions.

1 INTRODUCTION

The external jacketing by means of fiber reinforcement polymers (FRP) is known to be a reliable technique for improving the seismic capacity of deficient RC columns [Katsumata et al. (1988), Saadatmanesh et al. (1994), Nanni et al. (1995), Seible et al. (1997), Parvin et al. (2001), Ghali et al. (2003), Hadi (2006), Sadeghian et al. (2010), Kabir and Shafei (2012), Ghatte et al. (2016)]. In particular, the deformation capacity of existing RC members can be increased by using an external confinement with FRP along the entire member length or only at the member's end, where the plastic hinge region is located [Di Ludovico et al. (2008a,b)]. However, the number of tests results on deficient RC columns confined with FRP is still poor if compared with the number of columns test without external confinement.

In a performance-based approach, the prediction of the cyclic force-drift behavior and ductility improvement of FRP confined RC columns is fundamental. Several models are provided in literature for columns without external reinforcement, some [Ibarra et al. (2005) deterioration model, among many others] more complex than others (bilinear model). The basic knowledge required about FRP confined RC members are the force and corresponding drift ratio at yielding

and the ultimate drift ratio at conventional defined failure. However, predicting models available for evaluating the deformation capacity of FRP confined members have a low accuracy [Biskinis and Fardis (2013)], due to the lack of a large number of experimental data.

In the present study, the results of an experimental program carried out on RC columns strengthened with composites materials are presented and discussed. In particular, five cantilever RC columns with square cross-section were tested: one unstrengthened control column and four columns confined with one and two plies of CFRP sheets. The columns have been strengthened using a continuous wrapping at the fixed end, where the plastic hinge region is located. The specimens were cantilevers loaded with a low compressive axial load and subjected to cyclic horizontal displacements. The responses of the columns have been analysed in terms of failure modes and increased deformation capacity in case of external CFRP confinement. Particular attention has been focused on the increased deformation capacity (i.e. ultimate drift and ductility) due to the external wrapping with respect to control column. In order to investigate on the effectiveness of CFRP confinement in case of axial load and bending moment interaction, a detailed analysis related to the axial strains distribution along the fibers is reported in the paper.

2 EXPERIMENTAL PROGRAM

2.1 Specimens geometrical and mechanical properties

Five cantilever RC columns were designed with geometrical properties and reinforcement detailing as reported in Figure 1a. Each specimen had a square cross-section 300 x 300 mm reinforced with six 18 mm diameter deformed bars (longitudinal geometrical reinforcement ratio, $\rho = A_s/bh = 1.7\%$ with A_s total area of longitudinal steel reinforcement and b,h cross section dimensions). Transverse reinforcement was made of 8 mm diameter ties, spaced at 150 mm apart (a reduced spacing has been adopted in the zone of load application to avoid localized damages).

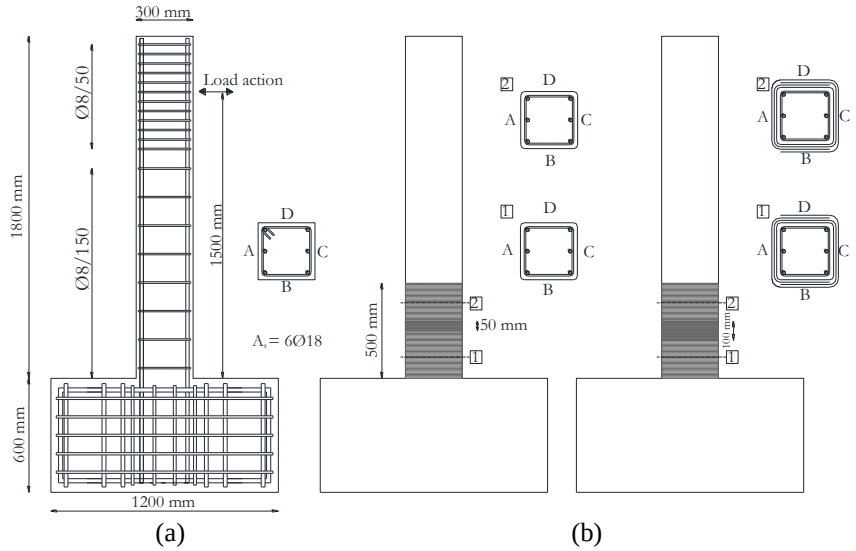

Figure 1. Geometry of specimens: control specimen (a) and confined configurations (b).

The lateral load has been applied at a distance of 1,500 mm from the base (i.e. L_s = 1,500 mm). Four specimens were confined at the column base with uniaxial CFRP sheets with fibers perpendicular with respect to the column longitudinal axis. The confinement was extended for 500 mm from the column-foundation interface. In particular, two columns (named F1 and F2) were confined with one layer of CFRP (unit weight 600 g/m^2). Since the width of CFRP sheets was 300 mm, two sheets have been used for the confinement, with a 50 mm vertical overlap region located at the mid height of the confined zone. The other two specimens (named F3 and F4) were confined with two plies of CFRP. The vertical overlap of sheets was 50 mm for each layer; at the mid height of the confined zone a total vertical overlap of 100 mm was attained. Two types of CFRP were used (named Type A and B), with mechanical properties reported in Table 1.
Two classes of concrete have been adopted: a low compressive strength for specimens F0, F1 and F2 and a medium compressive strength for specimen F3 and F4. Mechanical properties of materials are reported for each specimen in Table 2.

Table 1. Dry carbon fibers material properties.

CFRP type	*Unit weight* [g/m^2]	E_f [GPa]	ε_{fu} [%]	t_f [mm]
A	600	230	1.3	0.33
B	600	252	1.9	0.33

Table 2. Summary of the specimens material mechanical properties.

Test	f_{cm} [MPa]	ρ_f [%]	n° plies	CFRP type
F0	16.3	-	-	-
F1	14.9	0.22	1	A
F2	16.0	0.22	1	B
F3	29.1	0.44	2	A
F4	33.3	0.44	2	B

2.2 Test set-up and instrumentation

All the specimens were subjected to a constant compressive axial load ratio ($v = N / A_c f_c$, where N is the axial load, A_c is the concrete gross area and f_c is the mean cylindrical concrete strength) equal to 0.1 and a lateral cyclic loading under displacements control. The test setup and instrumentation are described in detail in Di Ludovico et al. (2013). A displacement rate of 0.2 mm/s was used for initial four cycles, then a higher rate 1.0 mm/s was adopted for the next five cycles and a rate 2.0 mm/s was used for the last cycles up to failure. In each cycle, the target displacement was achieved three times.

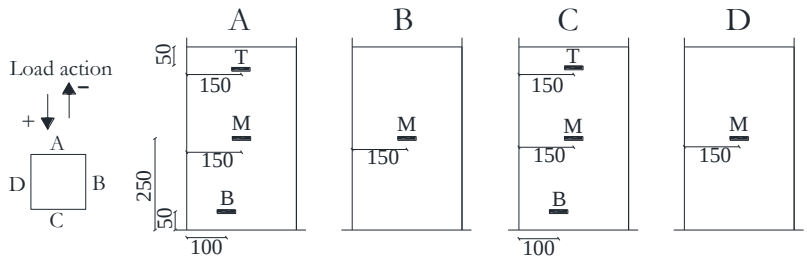

Figure 2. Strain gauges configuration for specimens F1, F2, F3 and F4 (dimensions in mm).

Strain gauges were placed on the composite material for monitoring the axial strains developed during the test. The strain gauges were located at Bottom (B), Middle (M) and Top (T) of the confined region for all confined specimens. The layout of strain gauges configurations on CFRP jacketing is shown in Figure 2. The strain gauges were placed at the mid-span of each side, except for the bottom ones, which were moved of 50 mm to the left in order to allow the LVDTs measurements.

3 DISCUSSION OF EXPERIMENTAL RESULTS

3.1.1 Failure modes and force-drift relationships

The control specimen, F0, developed a flexural behavior up to an imposed drift ratio ($\Delta = d/L_s$ with d equal to the horizontal displacement and L_s = 1,500 mm) of Δ = 6.4%, when a sudden drop of lateral strength was observed due to a shear-flexure interaction and the failure was achieved. At failure, large diagonal shear cracks were observed in the plastic hinge region and the concrete cover was completely spalled off (see Figure 3a); the spalling of concrete involved a region with a height of about 470 mm from the fixed end. At this stage, the buckling of longitudinal bars was also detected. Thus, the control specimen developed a "quasi-ductile" behavior, since a brittle mechanism (i.e. shear-flexure interaction) prevented the full attainment of the member plastic deformation capacity.

The brittle mechanism and the bars buckling were avoided in specimens confined at the column base with CFRP sheets, which experienced a pure flexural behavior. The confined specimens failure modes were governed by the concrete crushing inside the external jacketing; any CFRP tensile rupture or debonding phenomena have been observed during the tests. However, a premature failure mechanism given by horizontal cracks between fibers was detected in all specimens. In particular, longitudinal cracks along the fibers direction developed at about 50 mm from the column base due to a concentration of stresses provided in the direction orthogonal to the fibers by the totally crushed concrete, see Figure 3b. The shear-flexure interaction was prevented by increasing the shear capacity of the confined region. However, small diagonal shear cracks developed in unconfined region of the specimens (Figure 3b).

As expected, the CFRP external confinement did not increase the lateral capacity of specimens, subjected to low compressive axial load and cyclic uniaxial bending, but strongly enhanced their deformation capacity and relevant ductility. For better understanding the effectiveness of CFRP confinement on ductility enhancement, the experimental force-drift envelope curves for the five specimens are reported and compared in Figure 3c. Each envelope curve has been normalized with respect to the peak force achieved during the test by each specimen, F_{max}, in order to neglect the difference in concrete compressive strength. It should be noted that specimens F3 and F4 were characterized by concrete compressive strengths greater than other specimens (i.e.

f_{cm} = 29.1 and 33.3 MPa, about two times that of columns F0, F1 and F2) and confined with a higher ratio of external reinforcement (i.e. two plies of fibers instead of one). Thus, the theoretical increase of concrete ultimate axial strain due to external confinement is equal to that related to columns F1 and F2. Indeed, the confinement benefit in terms of increase of ultimate axial strain may be theoretically computed as a function of the ratio between the effective confinement pressure and the concrete compressive strength. A summary of experimental results in terms of ultimate drift ratio and ductility is presented in Table 3. The ductility has been evaluated from an equivalent bilinear curve: the yielding point is assumed as the intersection point between the secant line at 70% of the peak load and the horizontal line passing from the peak load.

The comparison among the five specimens response shows a very similar behavior for drift ratios ranging between 0 and ±4.8%, corresponding to the achievement of peak load for all specimens. After the peak, the control specimen F0 exhibited a fast degradation of lateral strength and stiffness up to the failure. A similar behavior was experienced by specimen F4, characterized by medium concrete compressive strength and confined with two plies of CFRP sheets. In this case, a slight increase of deformation capacity was observed (+12% and +25% in the positive and negative load direction, respectively).

The CFRP external confinement strongly increased the ultimate drift ratios for specimens F1, F2 and F3 with respect to the control specimen F0: +62% for test F1, +50% for test F2 and +50% (+40% in the negative direction) for test F3. In terms of ductility enhancement, μ, specimens confined with Type A composite material attained a greater increase of ductility due to the confinement effect (+68% for F1 and +75-91% for F3) with respect to specimens confined with Type B material (+54% and +72-89% for F2 and F4, respectively).

However, the enhancement in terms of ductility obtained by using two plies of CFRP instead of one is lower than 21% for specimens F1-F3 and lower than 35% for specimens F2-F4.

Table 3. Summary of experimental ultimate drift ratios and ductility.

		F0	F1		F2		F3		F4	
Δ_u [%]	(+)	6.4	10.4	+62%	9.6	+50%	9.6	+50%	7.2	+12%
	(-)	6.4	10.4		9.6		8.9	+40%	8.0	+25%
μ	(+)	4.3	7.2	+68%	6.6	+54%	8.2	+91%	7.4	+72%
	(-)	4.3	7.2		6.6		7.5	+75%	8.1	+89%

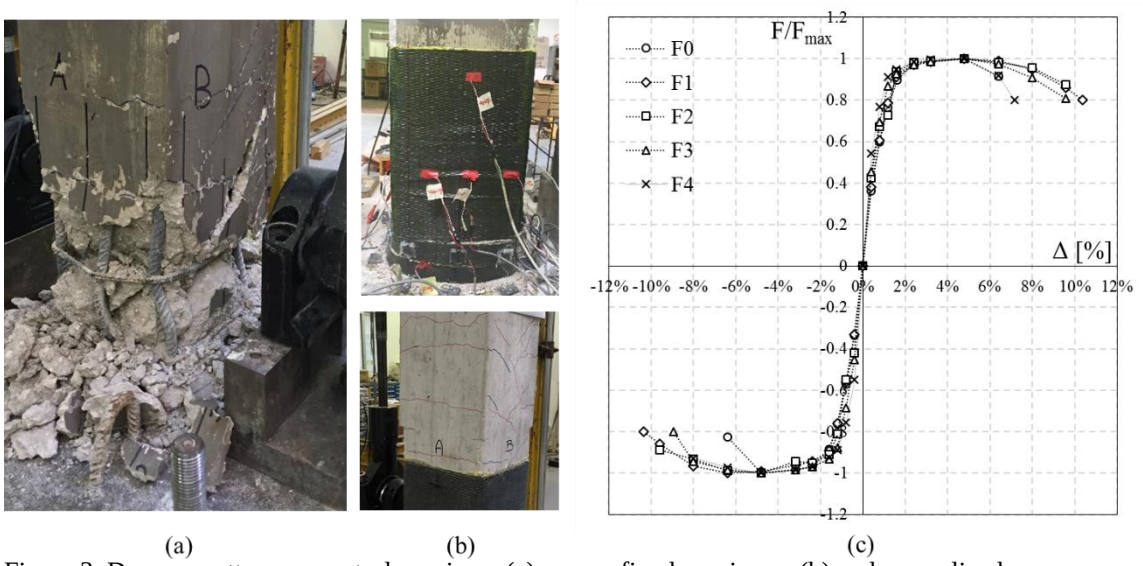

(a) (b) (c)

Figure 3. Damage pattern on control specimen (a), on confined specimens (b) and normalized experimental force-drift envelope curves for the five specimens (c).

3.1.2 Strain profiles

The axial strains developed in the CFRP confinement due to the concrete lateral dilatation in case of combined compressive axial load and uniaxial bending are investigated in this section.
The ratios between the recorded CFRP axial strains, ε_{CFRP}, and nominal CFRP ultimate strain, ε_{fu}, are presented for the specimen F1 as a function of the drift in Figure 5a,b for the positive and negative load action directions, respectively. In the positive load action direction (Figure 5a), the concrete in side C is subjected to axial compression whereas that in side A is in tension. Vice versa, in the negative displacement path (Figure 5b), concrete in side A is compressed and that in side C is in tension.
The carbon fibers axial strains recorded on the sides in tension-compression (i.e. sides A and C) resulted strongly greater than that recorded on the two column lateral sides (i.e. sides B and D), both in the positive and negative load action directions.

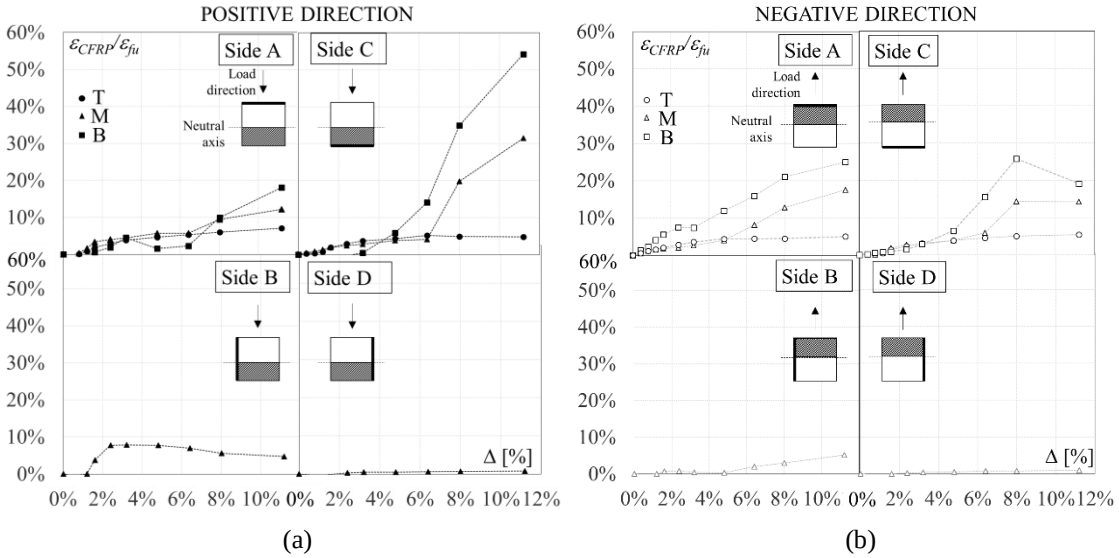

(a) (b)

Figure 5. Strain profiles for specimen F1 in positive (a) and negative (b) load direction.

This means that the strain transmission along the continuous fiber perimeter was not attained; the reason of such difference on the strain readings on sides parallel or orthogonal to the displacement action may be due to a corner stress/strain concentration, which avoided the diffusion of strains along the CFRP reinforcement.
A peak CFRP strain of 55%ε_{fu} was recorded at the bottom of the confined region, where the premature longitudinal cracks between fibers were developed. This peak represents a stress/strain concentration due to the concentrated lateral pressure generated by crushed concrete inside the fibers.
In the negative direction, the axial strains trend above the two sides in tension (C) and in compression (A) were comparable. Similar trends of strain profiles were observed for other specimens.

4 FIBERS EFFECTIVE STRAINS

For predicting the ultimate drift ratio of columns confined with FRPs, the most diffused procedure is based on the plastic hinge concept, associated to the calculation of cross-section curvatures at yielding and ultimate conditions.
In case of members confined with FRP, the moment-curvature analysis should be performed by assigning a specific stress-strain behavior for concrete confined with FRPs. However, stress-strain models for FRP confined concrete are usually derived from experimental tests on circular members under compression only and then extended to non-circular member subjected to axial load and bending moment. Those models for FRP confined concrete usually consider an effective axial strain uniformly distributed along the external jacket perimeter and equal to $\varepsilon_{f,eff} = k_{eff}\ \varepsilon_{fu}$, where k_{eff} is a reduction factor for limiting the maximum allowed fibers axial strain and for modelling the failure mode.
It should be noted that models based on pure compression experimental tests provide a fibers effective strain that could be very far from the fibers axial strains actually experienced during a cyclic test, where the actual distribution of axial strains is not uniform along the jacket perimeter.
Most of existing models for FRP confined concrete provided by international codes and recent literature give reduction factors k_{eff} derived from regression on experimental data. Only the ACI 440 (2008) limits the fibers effective strain based on considerations about the concrete core loss of integrity, as $\varepsilon_{f,eff} = min\ (0.004;\ k_{eff}\ \varepsilon_{fu})$, where the reduction factor k_{eff} = 55% is derived from experimental tests performd by Lam and Teng (2003).
Deriving the concrete stress-strain behavior for specimen F1 according to international codes formulations and most recent literature models [*fib* Bulletin 14 – Spoelstra and Monti (2001), ACI 440 (2008), CNR DT-200 (2013) [29], Biskinis and Fardis (2013), Pantazopoulou et al. (2016), Ghatte et al. (2016)], the fibers effective strain ranges between 31% ε_{fu} and 85% ε_{fu}, as reported in Table 4.

Table 4. Reduction factors for calculating the fibers effective strain according to different models.

	fib Bulletin 14 (2001)	ACI 440 (2008)	CNR 200 (2013)	Biskinis and Fardis (2013)	Pantazopoulou et al. (2016)	Ghatte et al. (2016)
k_{eff}	0.58	0.31	0.60	0.58	0.70	0.85

The use of proper fibers effective strains values is crucial for a correct prediction of FRP confined columns ultimate drift ratios; thus, a deep analysis of fibers strain profiles under cyclic loading and the analytical evaluation of experimentally found ultimate drift ratios will provide more indications about the prediction of FRP confined columns capacity.

5 CONCLUSIONS

The results of an experimental program carried out on five specimens subjected to combined axial load and uniaxial bending and confined with CFRP uniaxial sheets have been presented and discussed.

The confinement of the potential plastic hinge region prevented the development of a shear-flexure interaction mechanism and significantly increased the ultimate deformation capacity. In particular, the columns characterized by low concrete compressive strength and confined with one ply of CFRP increased the ductility of +54-68%, whereas the columns characterized by medium compressive strength and confined with two plies of CFRP increased the ductility of +72-91% with respect to the control specimen.

The distribution of CFRP axial strains along the cross-section perimeters, recorded by means of strain gauges, shows an evident strain gradient in all specimens tested. In particular, the fibers strains were greater above the two sides in tension/compression with respect to the lateral sides. Thus, the strain transmission along the continuous fiber perimeter was not attained, probably due to strain concentrations at corners. Beside the non-uniform strains distribution along the cross-section perimeter, a general increase of outer fibers strain has been recorded in the post peak phase, when the concrete cover is fully spalled off and the confined concrete starts crushing.

CFRP strain peaks were achieved at the bottom of the confined region, where the premature longitudinal cracks between fibers developed, both in positive and negative direction. In particular, a peak of 55% of the ultimate CFRP strain has been recorded near the longitudinal crack for the specimen confined with one ply of composite material. Experimental data on fibers axial strains during cyclic tests are useful for clarifying the modelling process of FRP confined concrete behavior under axial load and bending moment.

REFERENCES

ACI 440.2R-08, Guide for Design and Construction of Externally Bonded FRP Systems for Strengthening Concrete Structures, ACI: Farmington Hills, MI, USA, 2008.

Biskinis, D., Fardis, M.N., Models for FRP-wrapped rectangular RC columns with continuous or lap-spliced bars under cyclic lateral loading, *Eng. Struct*., 57, 199–212, 2013.

Consiglio Nazionale Delle Ricerche (CNR). Instructions for design, execution and con-trol of strengthening interventions through fiber-reinforced composites. CNR-DT 200-13, Consiglio Nazionale delle Ricerche, Rome, Italy; 2013.

Di Ludovico, M., Manfredi, G., Mola, E., Negro, P., Prota, A., 2008a, Seismic Behavior of a Full-Scale RC Structure Retrofitted Using GFRP Laminates. *Journal of Structural Engineering*, 134(5): 810-821.

Di Ludovico, M., Balsamo, A., Prota, A., Manfredi, G., 2008b, Comparative Assessment of Seismic Rehabilitation Techniques on a Full-Scale 3-Story RC Moment Frame Structure. *Structural Engineering and Mechanics*, 28(6): 727-747.

Di Ludovico, M., Verderame, G., Prota, A., Manfredi, G., Cosenza, E., 2013, Cyclic Behavior of Nonconforming Full-Scale RC Columns. *Journal of Structural Engineering,* 2013.

fib Bulletin 14. Externally bonded FRP reinforcement for RC structures. CH-1015, Lau-sanne, 2001.

Ghali, K.N., Rizkalla, S.H., Kassem, M.A., Fawzy, T.M., Mahmoud, M.H., 2003, FRP-Confined circular columns under small eccentric loading. *Proceedings of the Fifth Alexandria International Conference on Structural and Geotechnical Engineering*, December 2003, Alexandria, Egypt.

Ghatte, H.F., Comert, M., Demir, C., Ilki, A. (2016), Evaluation of FRP Confinement Models for Substandard Rectangular RC Columns Based on Full-Scale Reversed Cyclic Lateral Loading Tests in Strong and Weak Directions, *Polymers*, 8(9), 323.

Hadi, M.N.S. 2006, Behaviour of FRP wrapped normal strength concrete columns under eccentric loading. *Composite Structures*, 72: 503-511.

Ibarra L.F., Medina R. A., Krawinkler H. (2005), Hysteretic models that incorporate strength and stiffness deterioration, *Earthquake Engineering and Structural Dynamics*, 34(12), 1489-1511.

Kabir, M. Z., Shafei, E. (2012), Plasticity modeling of FRP-confined circular reinforced concrete columns subjected to eccentric axial loading, *Composites Part B: Engineering*, 43(8), 3497-3506.

Katsumata, H., Kobatake, Y. and Takeda, T. 1988, A study on strengthening with carbon fiber for earthquake-resistant capacity of existing reinforced concrete columns. *Ninth World Conference on Earthquake Engineering*.

Lam, L., Teng, J.G., Design-oriented stress-strain model for FRP-confined concrete in rectangular columns, *J. Reinf. Plast. Compos*, 22, 1149–1186, 2003.

Nanni, A. and Norris, M. 1995, FRP jacketed concrete under flexure and combined flexure-compression. *Construction and Building Materials*, 9(5): 273-281.

Pantazopoulou, S.J., Tastani, S.P., Thermou, G.E., Triantafillou, T., Monti, G., Bournas, D., Guadagnini, M., Background to the European seismic design provisions for retrofitting RC elements using FRP materials, *Structural Concrete*, 17(2), 194-219, 2016.

Parvin, A. and Wang, W. 2001, Behavior of FRP jacketed concrete columns under eccentric loading. *Journal of Composites for Construction*, 5(3):146-152.

Saadatmanesh, H., Ehsani, M.R., Li, M. W. 1994, Strength and Ductility of Concrete Columns Externally Reinforced with Fiber Composite Straps. *ACI Structural Journal*, 91: 434-447.

Sadeghian, P., Rahai, A. R., Ehsani, M. R. (2010), Experimental study of rectangular RC columns strengthened with CFRP composites under eccentric loading, *Journal of Composites for Construction*, 14(4), 443-450.

Seible, F., Priestley, M.J.N., Hegermier, G.A. and Innamorato, D., 1997, Seismic retrofit of rc columns with continuous carbon fiber jackets. *Journal for Composites for Construction*, 1(2): 52-62.